Chapter 5 - Comparison of the Chi Equation to Measurements

The purpose of this chapter is to first establish that the chi plot is in most cases an excellent analytical description of the various standard curves. Indeed it is now questionable that those standard curves which do not follow the chi plot are free from multiple energies of adsorption or from microporosity. Once this is established, then the chi theory (, disjoining theory or standard plot application since they are all equivalent) may be used to analyze various adsorption experiments, including heats of adsorption, microporosity, mesoporosity, heterogeneity, etc. Along with this will be presented some predictions and preliminary evidence that these predictions are correct. Additional details concerning the fits of the standard curves, regardless of these problems are given in the literature[1].

Comparison to Standard Isotherms

In chapter 3, a variety of standard plots was presented. It is instructive to plot these as chi plots to see how well they obey the analytical expression, In the following, the chi plot fits will be performed only on original data where available. Creation of the standard plot by some fitting routine or simply using a manual spline fit is in itself a distortion of the data. Indeed, the thoria and lunar soils standard plots were created using the insights of the chi plot, so the standard plot by definition must fit the chi plot perfectly. Similar problems are encountered in analyzing heats of adsorption.

In the analysis that follows, the slope of the fit, the χ intercept (χ_c), the standard deviation of the fit and the statistical *R* will be presented.

The α-s Standard Plots

The most widely used standard plot is the α-s plot created by Sing, et. al.[2], for both N_2 and Ar adsorption. The original data [3] is presented in **Figure 64** for argon adsorption and in **Figure 65**

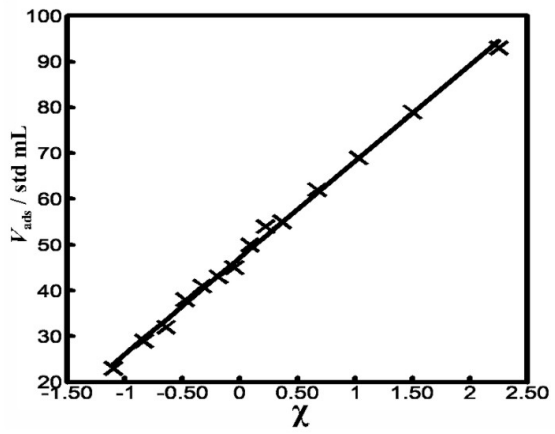

Figure 64 Argon adsorption on silica used to create the standard α-s plot as a chi plot. The line is the chi plot least squares fit.

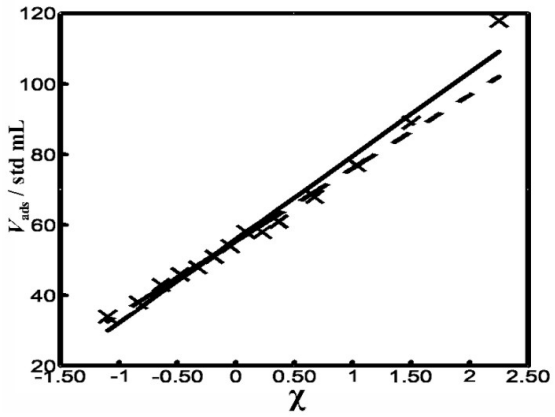

Figure 65 Nitrogen adsorption on silica used to create the standard α-s plot as a chi plot. The line is the least squares fit.

Table 28 Data from the α-s curves by Sing, et. al., of Ar and N_2 on SiO_2

α-s for Ar on SiO_2	α-s for N_2 on SiO_2	α-s for N_2 on SiO_2 *
Slope = 21.1 mL	Slope = 23.7 mL	Slope = 20.8 mL
n_m = 0.942 mmol	n_m = 1.057	n_m = 0.53 mmol
χ_c = -2.23	χ_c = -2.36	χ_c = -2.67
σ = 0.36 mL	σ = 1.09 mL	σ = 0.53 mL
R = 0.997	R = 0.975	R = 0.993

* fit for dashed line that leaves off the highest point.

for nitrogen adsorption. In **Table 28** is a summary of the data that can be extracted from these α-s plots.

For the N_2 adsorption the a second fit indicated by the dashed line in **Figure 65** was performed. As mentioned in the first chapter, occasionally the data at the high pressures, for a variety of reasons, may not be reliable. The most likely deviation is in the positive direction as seen here. Other silica data do not indicate this upswing. Therefore, an additional fit was performed leaving off this higher point. In **Table 28** the last column provides the fit with the highest data point not counted. The original data as shown here with the fit is judged to be more reliable than the smoothed α-s tables. It appears that in the smoothing process some inaccuracies were introduced.

Cranston and Inkley Standard *t* Curve

The *t* curve by Cranston and Inkley[4] is a fairly early standard curve. The data was an average curve for a variety of ceramic materials including alumina and silica. Given this, the statistics would seem to be meaningless, so they are not presented here. However, it is clear from **Figure 66** that the chi description is indeed a very good description of this standard plot. ($t = V_{ads}/\overline{A}$ or $t = 1.547\ V/A_{BET}$ for N_2 where V is the volume of the adsorbed gas as the gas state, not the adsorbed state.)

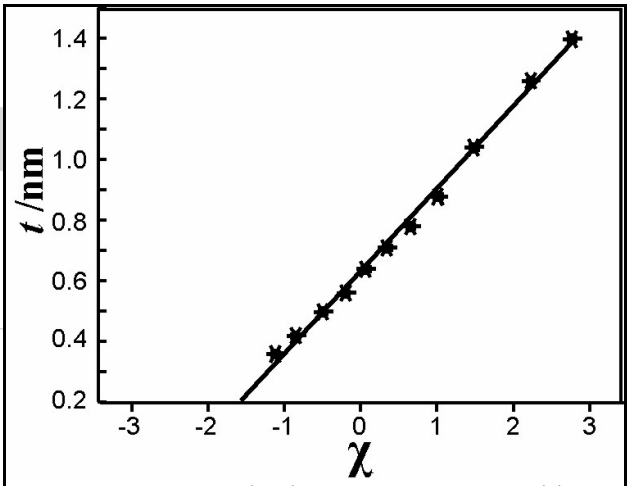

Figure 66 Standard *t* curve constructed by Cranston and Inkley. The data point by the authors. The line is the least squares χ fit.

deBoer's Standard *t*-Plots

deBoer, et. al., performed many experiments from which a standard *t*-plot could be constructed. These included most prominently the standard *t*-curve on alumina by Lippens, Linsen and deBoer[5]. (The calculation of the "thickness" value depends upon the BET calculation. The conversion used was

$$t - 3.53\times10^{-10}\left(V_{\text{ads}}/V_{\text{m, BET}}\right)\text{m} \qquad \textbf{(305)}$$

Where $V_{\text{m,BET}}$ is the STP gas volume of a monolayer according to the BET calculation. Even though the actual value for the monolayer equivalence is in question, for the present discussion this does not matter.) If the standard *t*-curve is plotted as a chi plot, a noticeable curvature is detected. If, however, the original data, available in the same series of papers by deBoer, Linsen and Osinga[6], is plotted, it is not so obvious that this curvature is real.

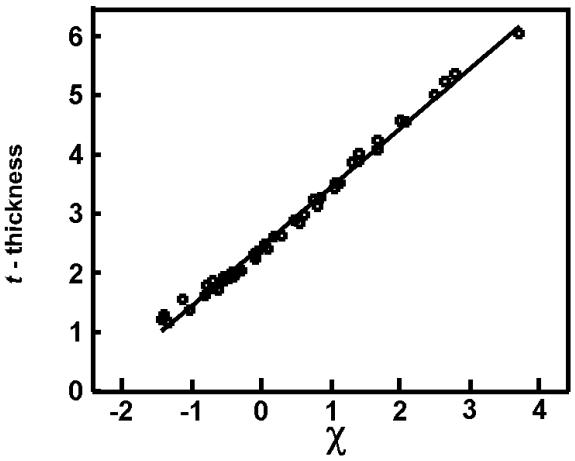

Figure 67 Standard *t* curve data by deBoer, Linsen and Osinga. The data are the circles and the line is the chi plot least squares fit.

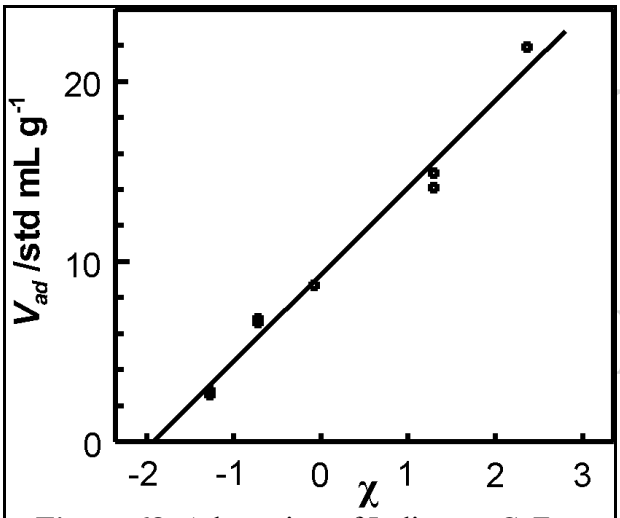

Figure 68 Adsorption of Iodine on CaF showing the chi plot relationship according to deBoer. This is one of the earliest observations of the chi relationship

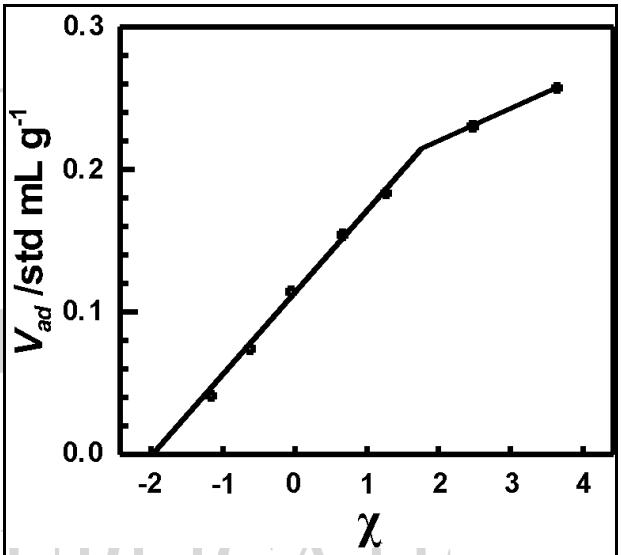

Figure 69 Adsorption of Ar on SnO according to deBoer and Zwikker. The roundoff in the upper portion is probably due to mesoporosity.

In **Figure 67** is the original data used to construct the *t*-plot of N_2 on graphitized carbon black.

The earliest plot of adsorbate versus -ln(-ln(P/P_{vap})) was proposed by deBoer which fit the adsorption of I_2 on CaF_2[7]. **Figure 68** is the illustration of this data in chi plot representation. It was recognized by deBoer at that time that the fit to the chi plot was very good.

Another example is that used by deBoer and Zwikker[8] to develop the polarization model[50]. This example is of argon adsorption on tin II oxide as shown in **Figure 69**. It appears, however, that this sample had some microporosity, however, the fit is very good up to quite a high value of χ.

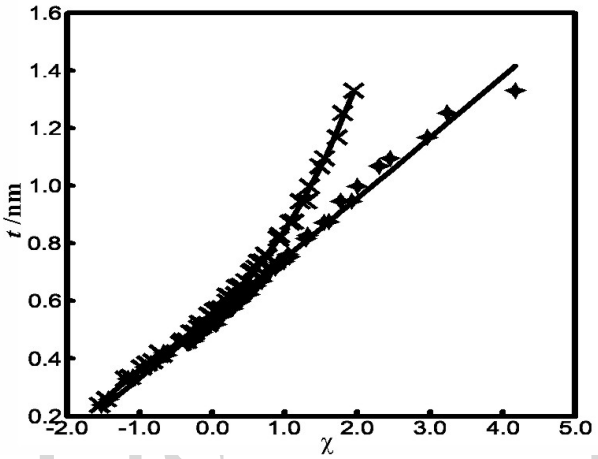

Figure 70 N_2 adsorption on MgO aerosil according to deBoer, Linsen and Osinga.

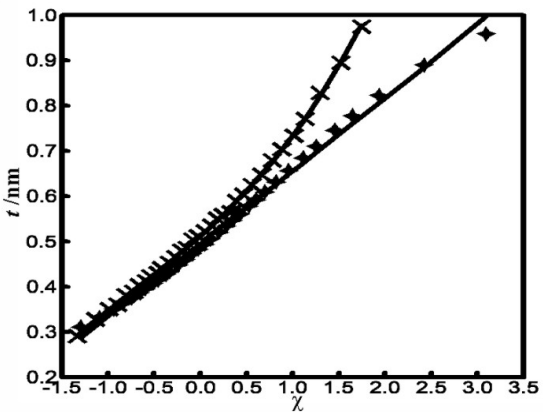

Figure 71 N_2 adsorption on Ni antigorite according to deBoer, Linsen and Osinga.

In addition to the well-known alumina adsorption, deBoer, Linsen and Osinga created standard plots for $BaSO_4$, TiO_2, ZrO_2, MgO, SiO_2-aerosil, Nickel antigorite, Graphon 1 carbon, Graphon 2 carbon and Sterling FT carbon. According to these authors, all but the carbon samples fit the standard t-curve well. Some examples chi plots of some of these are presented in **Figure 70** and **Figure 71**. All but the carbon samples had upswings at high pressures indicating possible in all likelihood as 1 K error in measurement as seen in many of the other data of the period.

The curves in **Figure 70** and **Figure 71** can be fit to within a maximum absolute error of 2% with the following third order coefficients given in **Table 29**. Increasing the power to the 4th power does not improve the fit. Assuming a typical 1 K radiative heating, a correction in **Figure 70** and **Figure 71** turns out to be nearly a straight line. The analysis for this is also given in **Table 29**.

[50] Empirically, this model, which plotted amount adsorbed versus **-ln(-ln(**P/P_{vap}**)** was a very good fit. However, after strong ridicule by Brunauer this model, called the polarization model, was abandoned. It is unfortunate that this happened since this held the field back from making advance in theory and quantitative analysis for at least 50 years.

Table 29 Parameters for the adsorption N_2 on MgO and Ni antigorite - a 3rd power fit and a chi fit with a ~1K temperature correction.

N_2 adsorbed on MgO				N_2 adsorbed on Ni antigorite			
power 0	0.554	$\chi_{c=}$	-2.590	power 0	0.512	$\chi_{c=}$	-3.052
power 1	0.225	$t_{m=}$	0.209	power 1	0.181	$t_{m=}$	0.162
power 2	0.049	R =	0.992	power 2	0.028	R =	0.998
power 3	0.020			power 3	0.012		

Standard Thoria Plots

One of the advantages that thoria presents is that it is very stable with respect to high temperatures. Once a thoria produced powder is high fired to 1600°C, it is virtually physically stable. The surface chemistry is also stable with no change in stoichiometry. It is therefore an ideal powder with which to perform basic research.

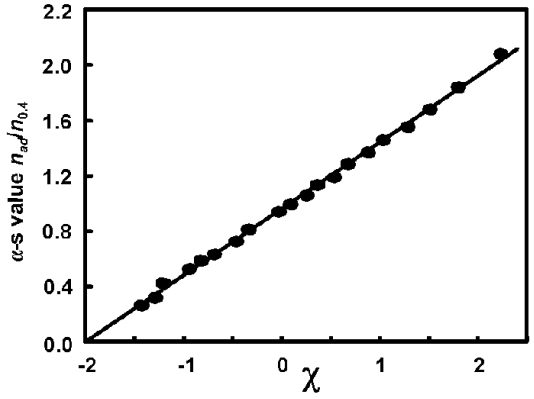

Figure 72 Nitrogen adsorption on thoria normalized to 0.4 P/P_{vap}. Data by Gammage, Fuller and Holmes

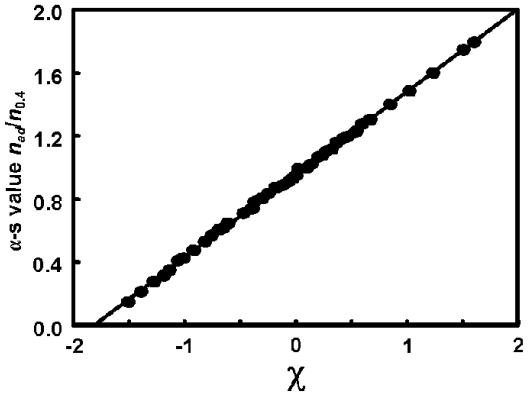

Figure 73 Argon adsorption on thoria normalized to 0.4 P/P_{vap}. Data by Gammage, Fuller and Holmes

Gammage, Fuller and Holmes[9] have performed extensive research on this material and have determined that for powders that are out-gassed at 1000°C there are several complicating features. Firstly, there is adsorption that is similar to chemisorption. This would be high energy adsorption sites in small micropores. Secondly, there is some mesoporosity and then thirdly, a normal non-porous flat surface adsorption. If the material is exposed to water and then degassed at low temperatures, one observes only the flat surface area. The isotherm for the high temperature out gas has been presented in chapter 4. What is of special interest is the analysis of the low temperature out-gassed material. The thoria had previously been out-gassed at 1000°C and then exposed to water vapor. The subsequent high vacuum degas was at 25°C. This treatment apparently covered the high energy areas and filled the microporosity so that only the outer surface area is in this case being measures. In **Figure 72** and **Figure 73** and are the N_2 and Ar adsorption plots. In these figures the data has been normalized to P/P_{vap} of 0.4 as one would do for an α-s plot.

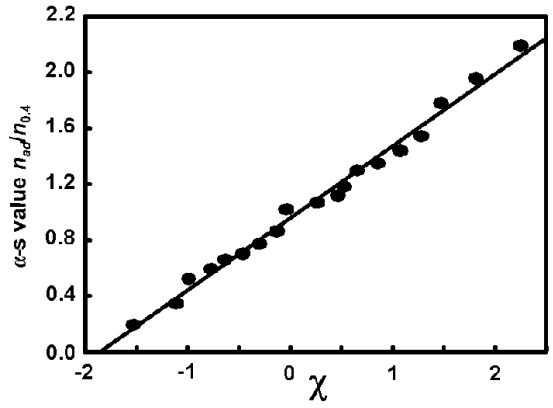

Figure 74 Adsorption of water at 25°C after several prior adsorption cycles. Data is normalized to 0.4 P/P_{vap}. Data by Gammage, Fuller and Holmes.

Even the water adsorption isotherm reveals a good fit to the chi plot. The plot in **Figure 74** is for water adsorption at 25°C on a powder that had been previously exposed to water seven times but had been out-gassed at 25°C for an extended period of time between exposures. For each exposure there was some additional irreversible adsorption. This would be the indication that the high energy planes and micropores were being masked for subsequent adsorption cycles. The fit to the linear chi plot in **Figure 74** is quite good.

In **Table 30** are the statistics for the three thoria adsorption isotherms.

Table 30 The statistics for the adsorption of gasses on 25°C out-gassed thoria.

	N_2 adsorption	Ar adsorption	water adsorption
Slope	2.60	2.81	2.45
σ	0.03	0.01	0.06
χ_c	-1.993	-1.816	-1.855
R	0.9992	0.9997	0.9948

The units for the slope and σ are relative α-s units, mol $mol_{0.4}^{-1}$.

Standard Curves for Lunar Soils

Lunar soils have the interesting property that they are well out-gassed. The soils were collected on the moon and placed in a well cleaned ultra-high vacuum aluminum alloy "moon box". The moon box was sealed on the moon with an indium seal. Upon arrival on earth the moon box was transferred to a very pure argon box and the soils transferred to smaller well-sealed containers for distribution. It is probably true that no sample, much less soil, has been handled in such clean and uncontaminating conditions. The soils obtained were of surprisingly uniform composition.

Several different isotherms were obtained. The chi plots for these are in **Figure 75** through **Figure 78**. One of the interesting features for the oxygen isotherm will be described in the section on the threshold pressure.

Apparently, due to the very clean and uniform conditions of the surface of these soils, the chi plots are very linear. In **Table 31** are the statistics for the lunar soil chi plot fits. The following data points were ignored for these fits: the first three data points for O_2 for an obvious reason and the last three data points for N_2 which seemed to be experimentally out of line.

Either from the graphs or from **Table 31**, it is obvious that the chi plot is an excellent description.

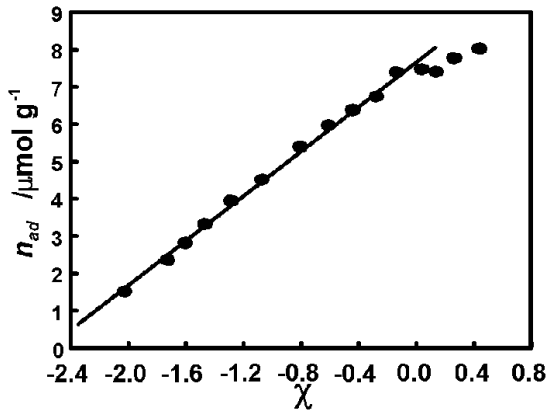

Figure 75 N_2 adsorption on lunar soil

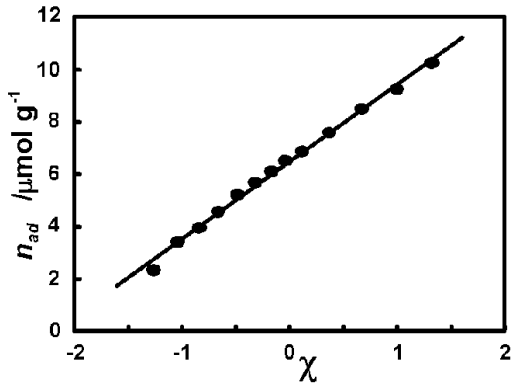

Figure 76 Ar adsorption on lunar soil

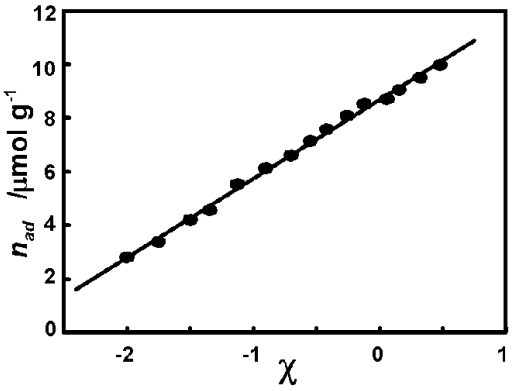

Figure 77 CO adsorption on lunar soil

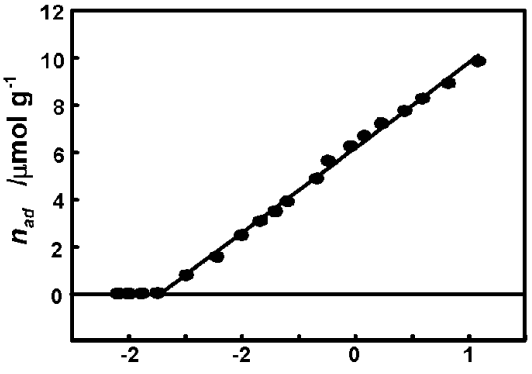

Figure 78 O_2 adsorption on lunar soil

Table 31 The statistics for the adsorption of gasses on lunar soil.

	N_2 adsorption	Ar adsorption	CO adsorption	O_2 adsorption
Slope	2.99	2.96	2.94	3.60
σ	0.06	0.06	0.05	0.06
χ_c	-2.564	-2.186	-2.951	-1.718
R	0.9977	0.9976	0.9984	0.9983

The units for the slope and σ are μmol g^{-1}.

Nicolan and Teichner[10] obtained several isotherms for various materials. They studied adsorption on non-porous silica and NiO. The chi plots of the adsorption on silica are presented in **Figure 79** and **Figure 80**. Although these indicate a nearly linear fit, the applicability is questionable since the lowest data point is more than a (postulated) monolayer of adsorbate. Furthermore the range of the data is, compared to the α-s data, relatively rather short. The data for the adsorption of N_2 on NiO is presented in **Figure 81**. Here the range of the data is better and the fit to the chi plot is also very good..

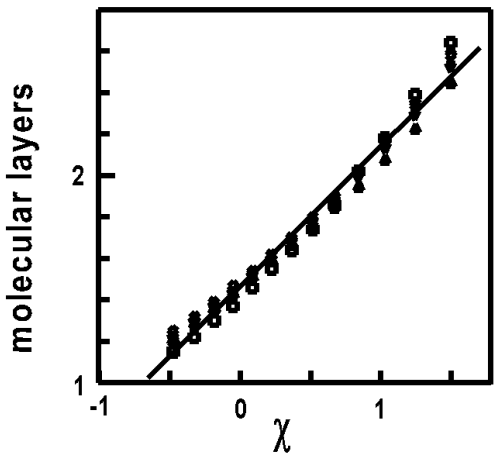

Figure 79 N_2 adsorption on SiO_2 by Nicolan and Teichner.

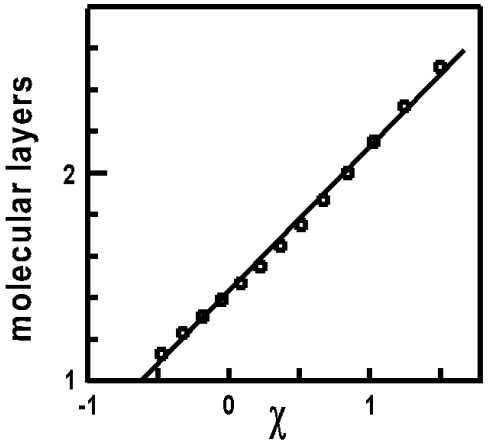

Figure 80 Ar adsorption on SiO_2 by Nicolan and Teichner.

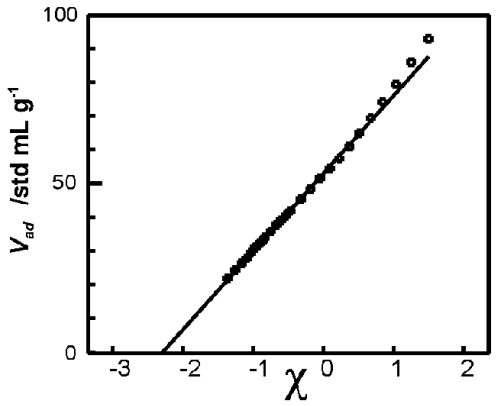

Figure 81 N_2 adsorption on NiO by Nicolan and Teichner.

The information with respect to the molecular layer cannot be analyzed due to lack of information to make the conversion, but the analysis for **Figure 81** is presented in .**Table 32**

Isotherms Quoted by Bradley

In addition to his own work[11],[12] of Ar adsorption on sulfate salts Bradley cited the work of McGavack and Patrick[13] of SO_2 adsorption on SiO_2 and water adsorption on CuO by Bray and Draper[14]. Although these data are quite old, there is no reason to suspect they are not accurate. Furthermore, they represent some rather unique isotherms which provide here a broader perspective. **Figure 82** and **Figure 83** are the isotherms of Ar on $CuSO_4$ and $Al_2(SO_4)_3$ by Bradley in the chi representation.

Table 32 Results of the χ plot fit.

N_2 adsorption on Ni - fig 18	
χ_c =	-2.271
n_m /mmol =	1.06
R =	0.997

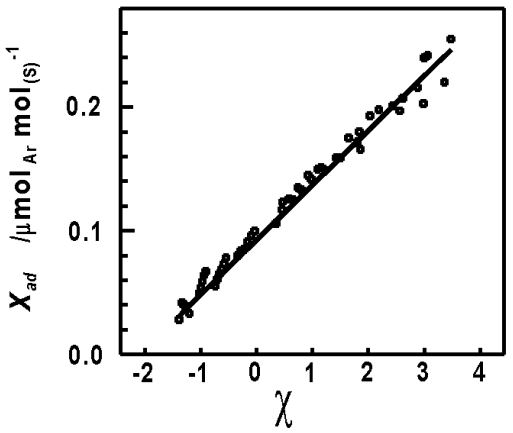

Figure 82 Adsorption of Ar on $CuSO_4$ according to Bradley.

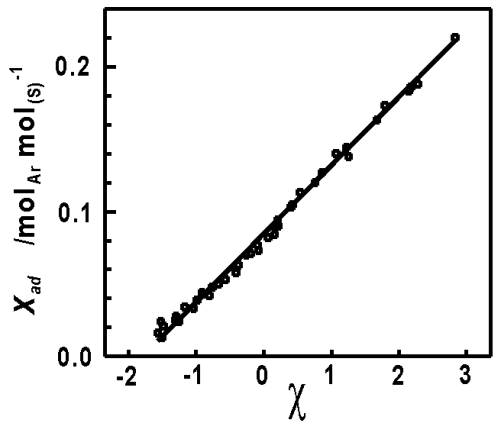

Figure 83 Adsorption of Ar on $Al_2(SO_4)_3$ according to Bradley.

For the adsorption of Ar on $CuSO_4$ several measurements were made at slightly different temperatures in an attempt to extract the isosteric heat of adsorption. One can see this in **Figure 82** by groupings of data with trends at the low adsorption end of the isotherm. The data by Bray and Draper of water on CuO and on a mix of 38.1 % MnO_2 and 61.9 % CuO show obvious evidence of porosity.

Bradley interpreted the data from McGavack and Patrick as consistent with the theoretical model for a standard. However, the original publication by McGavack and Patrick is much more extensive and more complex. Thus, separate section is presented here to discuss their results.

McGavack and Patrick[13]

The data may be represented quite well by a chi plot as may be discerned from and **Figure 84**. In these figures, three plots of adsorption of SO_2 on silica gel are shown at 0 °C with conditions as close as possible to each other but with different samples. When this is done, very good agreement was seen. The chi plots are very reproducible with similar E_as of about 15.0 (σ = 0.4) kJ mol^{-1}. Nearly all the isotherms produced good chi plots. However, when conditions were varied, for example temperature varied, there seems to be no correlations in the data. There was one very important conclusion regarding the contamination by either air or water. Contamination of the gas by 0.7 torr of air (for a 0 °C isotherm) lead to a hysteresis due apparently, as indicated by the chi plots, to a change in observed E_a. The addition of a percentage of water to the SO_2 gas phase had a similar result as demonstrated in **Figure 85**.

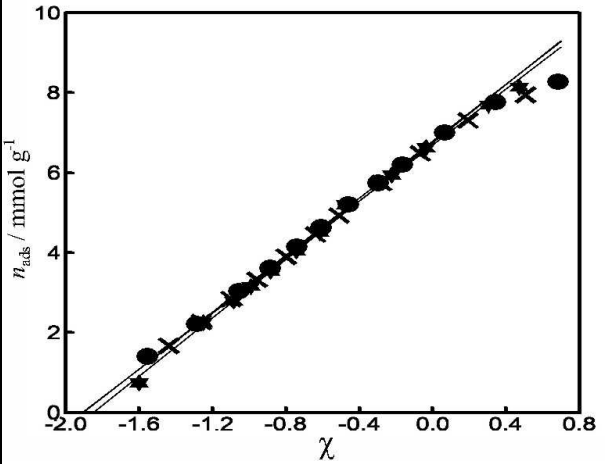

Figure 84 The chi plot representation of the adsorption of SO_2 on SiO_2 gel according to McGavack and Patrick. Three successive runs with identical condition with different samples.

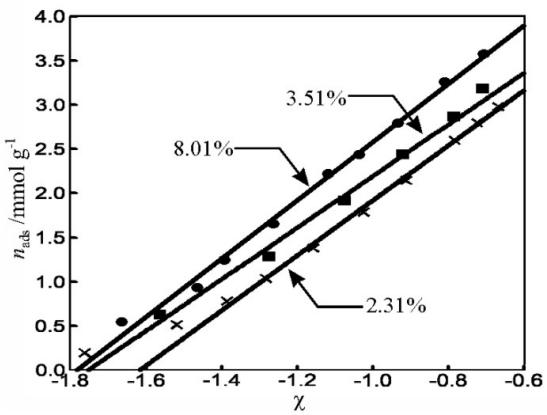

Figure 85 The effect water contamination of the SO_2 at three levels. It appears that the higher the H_2O level the higher is the apparent E_a.

Conclusion and some Comments about Carbon

From the discussion above it should be quite clear that the chi plot is at least a good empirical description for most simple isotherms. In constructing a standard isotherm, the fit to the chi plot would be the overall best choice. Numerous other examples could be cited with a variety of adsorbates-adsorbent pairs and an analytical expression for a standard curve could then be constructed.

It is however much more that just a standard curve. It frees one from the restrictions and uncertainties of the standard curve. As related in chapter 3 it allows calculations of microporosity and mesoporosity without the use of a standard and all the uncertainties attached with this approach. Furthermore, it provides a value for the surface area that is founded upon some very sound principles and reasonable assumptions.

There are several cases where more than one energy of adsorption must be dealt with. One of these is carbon. Most carbon samples have the additional complicating feature of microporosity. Apparently some carbon sample, such as the Sterling FT and Vulcan 3G do not have this complicating feature but still have more than one energy of adsorption. Indeed, one of these may be an in-register adsorption of either nitrogen or argon and has a very high adsorption energy.

Representative of such adsorption is the RMBM (Rodrigues, Martin, Prado and McEnaney,[15]) standard curve. Using the values of this standard curve and plotting them as a chi plot, as in **Figure 86**, one is able to see to two adsorption curves. The first one has a calculated energy of adsorption of about 45 kJ mol^{-1} which is very high for delocalized adsorption. The second one has a reasonable physisorption energy of adsorption of about 4.5 kJ mol^{-1}. The individual carbon curves have similar double fits. In general the low-energy (higher pressure) line is about the same for all the curves, whereas the energy of the high-energy portion varies from about 30 to 100 kJ mol^{-1}. This is an obvious indication that something other than simple physisorption is present.

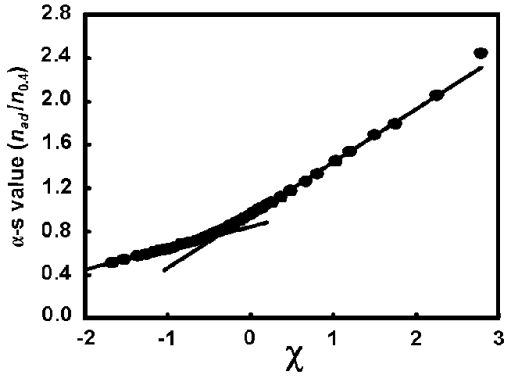

Figure 86 The RMBM standard α-s carbon curve.

The Observation of χ_c

The implication of χ_c is one of the most controversial aspects of chi theory. The presence of this parameter, which is related to the energy of adsorption of the first adsorbed molecule, implies that below some pressure of adsorptive there exists no adsorbate on the surface. (Again this is from a thermodynamic, i.e., large numbers, point of view.) In chapter 4 the argument was put forth that Gibbs' phase rule requires the presence of a threshold pressure. The theory that "Henry's law", in spite of the fact that it is hardly ever observed if one does not count the other Freundlich isotherms as "Henry's law", must be present is easily disproved by only one observation of the threshold pressure. It should be emphasized at this point that "Henry's law" for adsorption is not derivable from nor is it required by thermodynamics. "Henry's law" for adsorption is a postulated equation of state just as is, for example, the ideal gas law is for gasses. It is a result of the Langmuir isotherm, however, the Langmuir isotherm was formulated for chemisorption in which case a new component is created in the process which in turn changes the values in the Gibbs' phase rule. If the material on the surface is the same component as in the gas, then the Langmuir isotherm is not relevant. These arguments, however, do not seem to carry much weight so in this section are presented some examples where there is clear evidence of a threshold pressure.

There are three reasons that the threshold pressure has not been recognized in the past. Firstly, researchers knowing that "Henry's law" should be obeyed have not looked for a threshold pressure. Indeed, there are many incidences in the literature where an extrapolation is performed on the data to include 0.0 and most computer programs for instruments likewise perform this extrapolation. Secondly, most adsorbents studied are ceramic materials which have a fairly high energy of adsorption. The threshold pressure for these materials is typically below a P/P_s of 1×10^{-6}, below the normal measurement range. An extrapolation from 0.001 of P/P_{vap} to this value appears no different from an extrapolation through 0.0. (In other words, precisely speaking

the threshold pressure is insignificant.) The third reason is that many samples have heterogeneous surfaces or are contaminated with a variety of chemisorbed species thus giving the appearance of a heterogeneous surface. With a heterogeneous surface, an energy distribution is obtained that obscures the threshold effect. The calculations in chapter 4 demonstrated this.

The first evidence for the existence of χ_c is the direct observation of the phenomenon.

Firstly, there is some indirect evidence for the presence of χ_c , which is the energy consideration.

Observations of the Energy Implications of χ_c

The value of χ_c is related to an energy, E_a , by the equation:

$$E_a = -kT\,\mathbf{e}^{-\chi_c} \qquad \textbf{(306)}$$

where E_a is interpreted to be the energy that the first adsorbate molecule for any particular patch of surface releases upon adsorption. It is also related to the threshold pressure:

$$E_a = kT\,\mathbf{ln}\left(P_t/P_s\right) \qquad \textbf{(307)}$$

A discussion of how this energy is related to the substrate and the adsorbing gas has been given elsewhere[16]. Intuitively, one would expect this energy to be a function of both the gas and the solid. The expected trends for the value of $-E_a$ would follow:

- For adsorbing gases the expected trends should follow the values of the dipole moment, polarity, etc. Thus, one expects for $|E_a|$: $H_2O > CO_2 > N_2 > O_2 > Ar > He$
- For solids one expects the trend to follow the energy of a cleaved surface of the material (also follow the trend in surface dipole moments, etc.) Thus, one expects, for example: ThO_2 > MgO > Polystyrene > polytetrafluoroethylene (Teflon®)

For a series of compounds, such as oxides, the trend in $|E_a|$ should follow closely the enthalpies of the compound formations. The reason for this is that the higher the $\Delta_f\mathbf{H}^{\ominus}$s the more polarized are the oxide ions. Thus, for the following oxides the trends would be given as:

$UO_2 \approx U_3O_8 > Y_2O_3 > Al_2O_3 > ThO_2 > SiO_2 > BeO > H_2O > CO$

Experimental observation of such a trend in $|E_a|$ would be a strong indication that the threshold phenomenon is real. In **Figure 87** are the results of nitrogen adsorption on the above-mentioned oxides most of which were reported by Fuller and Thompson[17]. (H_2O

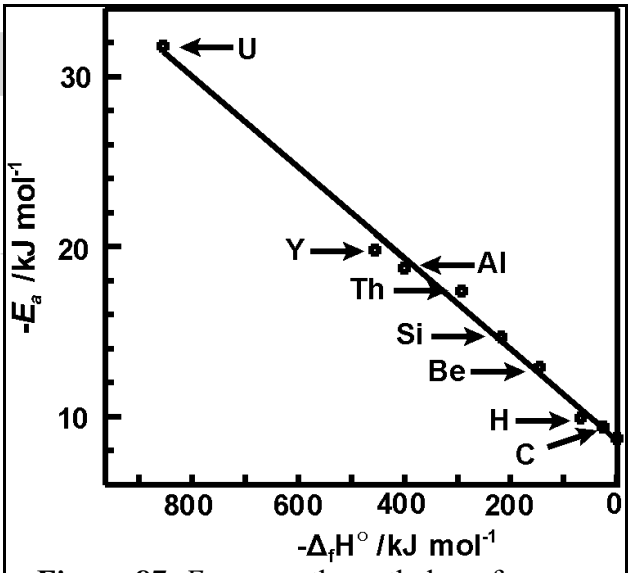

Figure 87 E_a versus the enthalpy of formation of various oxides.

is for water pre covered oxides and CO is for partially oxidized carbon.) The value for E_a of oxides is plotted as a function of the enthalpy of their formation. Since the threshold pressures for some of the oxides are too low to be measured directly, χ_c values obtained from the chi theory equation. It is apparent that the correlation does exist as predicted. Although not claimed, due to the question of stoichiometry to be used for the cleaved solid surface, this figure shows a linear relationship between the energies of the threshold and the enthalpies of formations. For the intersection at $\Delta_f\mathbf{H}^{\ominus} = 0$, the value for E_a should be that expected for the liquefaction of N_2. The data point on this axis represents a surface whose energy is such that there is no preference for liquefying on the surface. A fit for the data yields a value of 8.6 kJ mol^{-1}, which is somewhat high but in qualitative agreement.

Direct Observation of χ_c (threshold pressure)

In this section, to satisfy the disproof of "Henry's law" several instances of the observed χ_c are presented. This has indeed been reported in the literature by others. With the adsorption of water on NaCl reported by Peters and Ewing[18],[19] the threshold pressure is very clear, confirmed by both the isotherm and by infrared. In their investigation of the microporosity of Y-zeolites for which very low pressure measurements were needed Guo, Han, Zou, Li, Yu, Qiu and Xiao[20] reveal threshold pressures along with the reported oscillating adsorption. The oscillations are undoubtedly due to a variety of effects but one of these could be change in E_a .

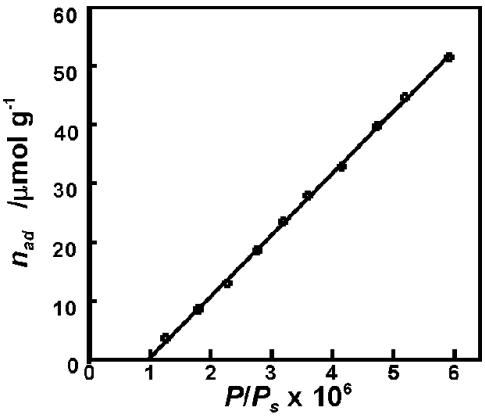

Figure 88 The observation of a threshold pressure by Gil, de la Puente and Grange with microporous carbon.

Gil, de laPuente and Grange[21] present data which seem to evidence a threshold pressure for N_2 adsorption. This observation was for nitrogen adsorption on microporous carbon. What is important about this data is that the threshold pressure is obvious even when looking at the data from the point of view of Henry's law. **Figure 88** illustrates this quite well. This plot illustrates that the threshold pressure is not an artifact of the transformation to the chi plot. In this figure the threshold pressure appears to be at about 1.0 x 10^{-6} P/P_s; whereas, a chi plot indicates it to be about 1.2 x 10^{-6} P/P_s.

In an attempt to observe the threshold pressure, Thompson selected a material that one would believe to have a low energy of adsorption. The direct

Table 33 Data for the adsorption of Ar on polytetrafluoroethylene (Teflon®)

P/P_{vap}	m_{ad} /g g^{-1}	P/P_{vap}	m_{ad} /g g^{-1}
0.000003	0.0x10^{-8}	0.053560	2.40x10^{-7}
0.000023	0.0x10^{-8}	0.099731	4.00x10^{-7}
0.000129	0.0x10^{-8}	0.159684	6.80x10^{-7}
0.001273	0.0x10^{-8}	0.299779	1.12x10^{-6}
0.004805	0.0x10^{-8}	0.399902	1.36x10^{-6}
0.008105	0.0x10^{-8}	0.599674	1.84x10^{-6}
0.015051	0.0x10^{-8}	0.698356	2.20x10^{-6}

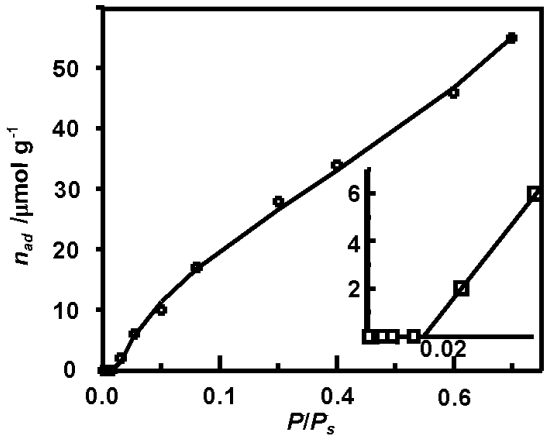

Figure 89 Ar adsorption on polytetrafluoroethylene (Teflon®) with the normal P/P_{vap} axis by Thompson.

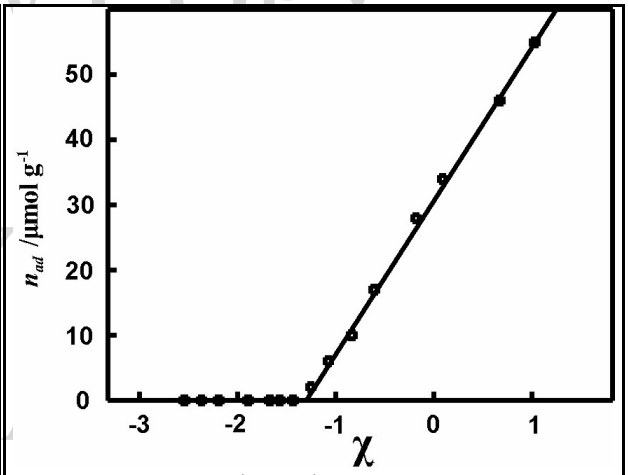

Figure 90 Ar adsorption on polytetrafluoroethylene (Teflon) using the χ axis by Thompson

observation of the threshold pressure is possible if the interaction energy between the surface and the adsorbed molecules is small. This can be easily illustrated with adsorption of N_2 or Ar on polytetrafluoroethylene (Teflon®) obtained by Thompson[22], which according theory should have a very high threshold pressure. The threshold pressure may clearly be seen at a pressure of about 0.01 atm (about 8 torr), well within (by a factor of at least 10^5) the capability of the most modern instrumentation. Direct observations of threshold pressures which are lower require the use of more sensitive gravimetric techniques. This was also found experimentally by Thompson with adsorption data on diamond and alumina that had an ultrahigh vacuum surface cleaning. Since the results of Thompson's polytetrafluoroethylene experiments have not been reported in the open literature, these will be discussed in some detail.

The powder used was a Teflon® Dupont resin obtained from Aldrich Chemical Company (polytetrafluoroethylene lot #6). The measurements on this material were performed over an extended period of time in both the adsorption and desorption mode. There was absolutely no indication that the isotherms exhibited any type of meta-stable condition or that the phenomenon reported herein is related to kinetics. The kinetics of both adsorption and desorption were indeed measured. The adsorption measurements and the desorption measurements were in agreement after the kinetic stage. What is shown here are only the stable thermodynamically valid portions of the measurements.

The results of the adsorption Ar on Teflon® shown in **Figure 89** are in the untransformed form to illustrate the shape of the isotherm. The data for this figure are given in **Table 33** to show the precision and accuracy that are obtainable with the instrumentation described. In this form, even with a high threshold pressure, the presence of a threshold pressure for most experiments, especially the volumetric type, would be missed. The zero pressure recording however is very obvious with the instruments described. This value is well within any conceivable error by a factor of 10^5. The flat portion of the pressure curve is more evident in the chi plot. This plot is shown in **Figure 90**. Here the presence of the threshold pressure becomes very obvious. This is very strong confirming evidence for the validity of the chi theory with respect to the threshold

phenomenon. In light of this first experiment that reported a threshold pressure, the theories based upon "Henry's Law" are disproven.

A variety of isotherms were obtained and the experiment repeated several times. In **Figure 91** are some data for three different types of experiments. For the low coverages, a slight rounding off of the chi equation plot is apparent as seen in **Figure 91**. However, the threshold pressure still exists well above the limit of detection. This rounding phenomenon may be attributed to the heterogeneous nature of the surface energy. The threshold pressure with this rounding is also seen with some other common standard isotherms.

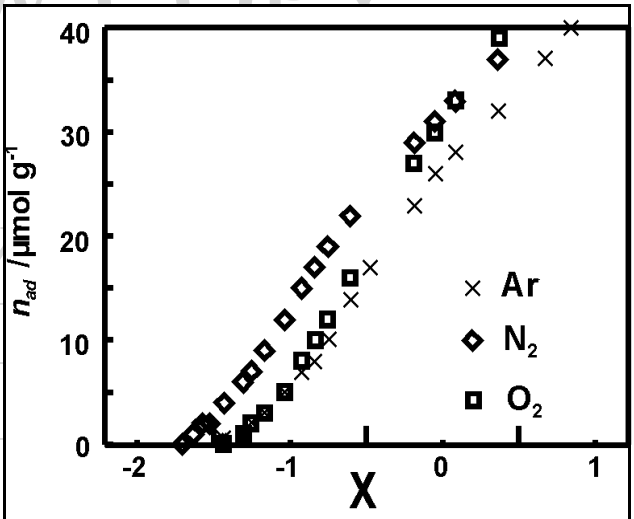

Figure 91 Various adsorption isotherms on polytetrafluoroethylene (Teflon®)

Similar threshold behavior is also apparent for both well cleaned diamond and alumina surfaces only at lower pressures. The results of these experiments are available in the open literature from a conference proceedings[23]. Thompson performed several experiments on these materials to test the hypothesis that a uniform surface may be created by a good ultrahigh vacuum cleaning, thus simulating the possible conditions that the lunar soils had. Heating in hydrogen at a high temperature and degassed under an ultrahigh vacuum created the right conditions to observe a threshold pressure for the argon adsorption isotherm.

Some of the details of the experiment are as follows. The diamond powder was 1 µm powder obtained from Amplex Corporation. This powder was degassed and heated in H_2 to obtain a clean surface. It is well known that heating in H_2 up to 1000°C can eliminate the graphitic carbon that often contaminates diamond surfaces, but there should also be other chemically bonded contaminates. The alumina powder was NBS 8571 which was cleaned in a similar manner. Entirely different isotherms for both materials are obtained if the out gassing step is performed in a different fashion. According the Smirnov, Semchinova, Abyzov and Uffmann[24], such a difference in surface structure with diamond may be due to the variation of the radicals on the surface. On the other hand, alumina may become slightly substoichiometric on the surface. **Figure 92** and **Figure 93** contain the results of the adsorption isotherms in the chi plot form on these materials. A very important observation was made with these materials. When the surfaces were contaminated, the threshold was not as apparent. Indeed, for diamond the adsorption isotherm followed the in-register chi

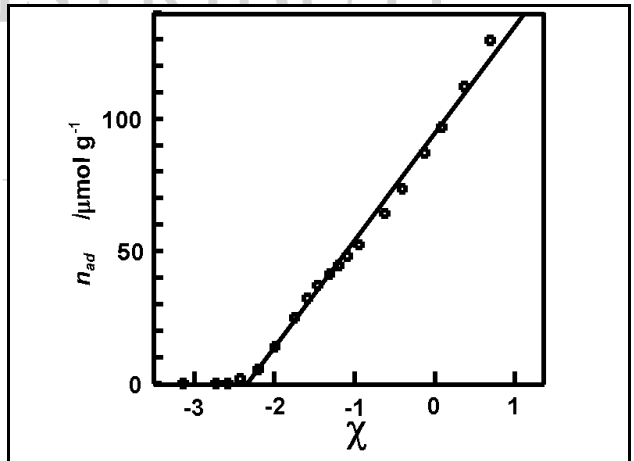

Figure 92 Chi plot of argon adsorption on diamond that has been cleaned in hydrogen. Data by K. Thompson.

theory analysis. This is probably due to the contamination creating a number of high-energy adsorption sites on the surface, thus masking the threshold effect. The hydrogen treated alumina evidences a threshold pressure; whereas, normally alumina chi curves, of which there is an abundance in the literature some of which are presented in this book, do not go to low enough pressures to observe this. The hydrogen treatment, which could yield a substoichiometric surface, apparently creates a lower energy of adsorption for nitrogen on alumina.

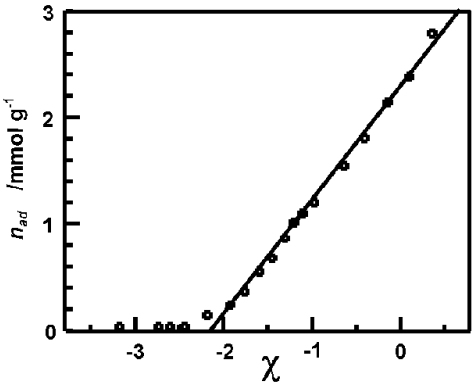

Figure 93 Nitrogen adsorption on hydrogen cleaned alumina. Data by K. Thompson.

In **Figure 78** the chi plot for the adsorption of oxygen on lunar soils was presented. It should be noted that the adsorption of oxygen below a χ-value of -1.72 was nonexistent. This was indeed observed for this material and was not an error in measurement. Thus, well-cleaned soil from the moon exhibits the threshold phenomenon with oxygen are at a relative high value of P/P_{vap} , i.e., about $P/P_{vap} = 0.0038$. Whether the other adsorbates would have exhibited such a clear threshold is unknown since the value of χ_c was below the detection limit.

Direct Observation with High Resolution Data:

Confirmation of χ_c has been provided with hight resolution isotherm measurements by J. Silvestre-Albero, A. M. Silvestre-Albero, P. L. Llewellyn and F. Rodrigues-Reinoso [25]. In addition to providing the evidence for the threshold pressure, this article is important for fore other reasons:

- It demonstrates the importance of High-resolution isotherms which extend into at least the high vacuum range.
- It demonstrates that helium calibrating gas used before the adsorption isotherm with the adsorbate gas is used distorts the isotherm. The calibration with He should be performed after the isotherm. This is probably a surprise to many investigators.
- The amount versus the log scale of P/P_{vap} is observed to monolayer restricted porosity, thus confirming one aspect of the chi theory.
- The validity of isotherms that depend on the existence of Henry's Law are disproved.

This article probably one of the most important articles published in the last ten

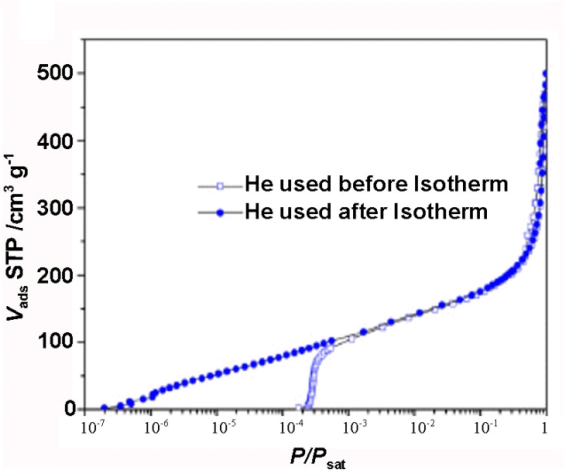

Figure 94 High-resolution N_2 adsorption isotherms at 77.4 K an activated carbon LMA233 on a logarithmic scale

years regarding physical adsorptionl. A few figures from this publication are shown here as **Figure 94** and **Figure 95** for adsorption of N_2 on carbon LMA223 and activated carbon DD52. Both of these are thought to have microporosity.

The plots are **log(*P*)** versus amount adsorbed. This is what is expected according to χ theory if the pores are of the size that only a singe monolayer can be adsorbed. (See page)

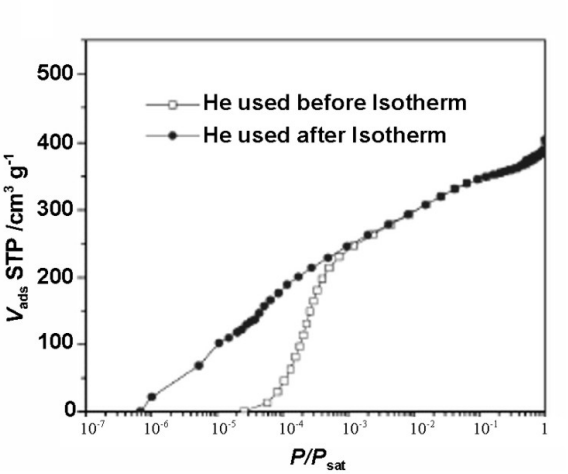

Figure 95 High-resolution N_2 adsorption isotherms at 77.4 K an activated carbon DD52 on a logarithmic scale

Conclusion Concerning χ_c

As mentioned previously, in order to disprove the universality of "Henry's law" one needs to present only one example of a threshold pressure. Several examples have been presented above so the disproof is complete.

Along with the observation of the threshold pressure the indirect evidence of the energy implications was also presented. The prediction of both the threshold pressure and energy implications is very strong supporting evidence for the validity of the chi theory. The predictions of the isosteric heats of adsorption, calculations of porosity, measurements of multiple plane adsorption (with its additive nature) and calculations of binary adsorbate mixture are not only supporting evidence but are quite useful. It is certainly an improvement over the BET which is theoretically weak and predicts very little.

Multiplane Adsorption

The terminology "plane" and "multiplane" here are used in the sense that there are distinct areas with differing E_as. These may indeed be different crystallographic planes, but adsorption experiments cannot determine this. The different E_as may be due to other factor such as, for example, microporosity. In the case of a distribution it may be due to a multiplicity of chemical species on the surface or contamination.

Examples of Two Plane Adsorption